NASA CR - 112194

ROTOR BLADE BOUNDARY LAYER MEASUREMENT

HARDWARE FEASIBILITY DEMONSTRATION

By David R. Clark and Thomas D. Lawton

Prepared under Contract No. NAS1-11213 by
Sikorsky Aircraft
Division of United Aircraft Corporation
Stratford, Connecticut 06602

for

NATIONAL AERONAUTICS AND SPACE ADMINISTRATION
Langley Research Center

NASA CR - 112194

ROTOR BLADE BOUNDARY LAYER MEASUREMENT

HARDWARE FEASIBILITY DEMONSTRATION

By David R. Clark and Thomas D. Lawton

Prepared under Contract No. NAS1-11213 by
Sikorsky Aircraft
Division of United Aircraft Corporation
Stratford, Connecticut 06602

for

NATIONAL AERONAUTICS AND SPACE ADMINISTRATION
Langley Research Center

ROTOR BLADE BOUNDARY LAYER MEASUREMENT

HARDWARE FEASIBILITY DEMONSTRATION *

By David R. Clark** and Thomas D. Lawton**

SUMMARY

A traverse mechanism which allows the measurement of the three dimensional boundary layers on a helicopter rotor blade has been built and tested on a full scale rotor to full scale conditions producing centrifugal accelerations in excess of 400g and Mach numbers of 0.6 and above. The mechanism weighs 0.29kg and can move a probe through an active range of 2.5 cm. Boundary layer velocity profiles have been measured over a range of rotor speeds and blade collective pitch angles. A pressure scanning switch and transducer were also tested on the full scale rotor and found to be insensitive to centrifugal effects within the normal main rotor operating range. The demonstration of the capability to measure boundary layer behavior on helicopter rotor blades represents the first step towards obtaining, in the rotating system, data of a quality comparable to that already existing for flows in the fixed system.

INTRODUCTION

Development of analytical methods for the understanding of boundary layer problems has generally been paralleled or preceded by an expansion of the available experimental data base. This is especially true when turbulent flows are being considered because of the random nature of the boundary layer velocity field and the open form of the defining equations. Closure has only been possible through the use of turbulence models based on the results of a few experiments carried out under controlled conditions.

Most experimental data on developing boundary layers has been obtained in circumstances where the mean flow was two dimensional. More recently, data has become available on configurations where the flow is markedly three dimensional. The data obtained on swept wings in reference 1 is typical. Little or no data is available, however, on flows where the effects of rotation are present and which could have some bearing on the development of analytical methods for calculating the boundary layer growth on helicopter rotors.

---

* The contract research effort which has led to the results in this report was financially supported by USAAMRDL (Langley Directorate)

** Aeromechanics Branch, Sikorsky Aircraft, Division of United Aircraft Corporation, Stratford, Connecticut 06602.

Significant exceptions to this are the studies of references 2 and 3 which examine the flow over spinning discs and in reference 4 which considers the flow over a helical surface of low pitch angle. The flow in all these examples, although rotation effects are present, is different from the rotor blade flow since in each case the boundary layer flow is predominately radial. This contrasts with the rotor blade which, with its well defined leading edge and short chord, has predominately tangential flows.

Despite the absence of any significant body of experimental data on rotor blade boundary layers, several workers have developed solutions for the three dimensional boundary layer problem including the effects of rotation. Most significant of the early studies are those presented in references 5 and 6. More recent work includes the unsteady laminar flow solution in reference 7, further exploration of the flow field in references 8 and 9 and a development of methods for solution of the turbulent compressible flow in reference 10. The one common factor between all the approaches was that assumptions had to be made regarding the basic characteristics of the flow because of the lack of experimental data.

Although measurement of boundary layer behavior in two dimensions, or even three dimensional non-rotating flows, presents no special problem, obtaining high quality data in a rotating system is a considerable task. Traverse mechanisms conventionally mounted outside the surface have to be contained within the rotating element (except in the special case of the spinning disc where polar symmetry exists) and the mechanism must be able to operate in the very high centrifugal accelaration fields met in practice. Accelerations as high as 400 g are common in main rotor applications and for tail rotors values in excess of 1000 are not uncommon. Any traverse mechanism for this application must consequently be small and very rugged.

Early investigators of the boundary layer on rotor blades confined themselves either to measurements of only the surface flow, with thin film heat transfer gauges, or to measurements at fixed positions above the surface. The work of references 11 through 14 is typical. To obtain a boundary layer velocity profile using a fixed probe requires a considerable expenditure of time. The probe is initially set at a desired height above the surface using some optical device. The rotor is then run up to speed, stabilized and the data taken. The rotor is then slowed and stopped and the probe reset. The whole cycle is repeated until enough data points have been taken to give a velocity profile. This method is obviously open to degradation of the data through poor repeatibility of conditions from one test point to the next.

To obtain data in a rotating system of quality comparable to that obtained in a well controlled, non rotating test the measurement must be carried out in as short a period of time as possible, ideally with only one speed setting of the rotor. To do this a blade mounted traverse is required and the development and demonstration of such a mechanism was the prime object of the present program.

SYMBOLS

C	hot wire cooling velocity. ie, the velocity perpendicular to the wire axis
u	chordwise velocity in boundary layer
U_∞	chordwise velocity outside boundary layer
v	spanwise velocity in boundary layer
z	distance normal to local surface
δ	boundary layer thickness. ie, height above the surface at which $u = 0.995\ U_\infty$
θ_{75}	rotor collective pitch (at 75% radius)

subscripts

1	hot wire identification number, inboard
2	hot wire identification number, outboard

DESCRIPTION OF TEST FACILITY

Whirl compatability testing was carried out on the Sikorsky Aircraft 3000 HP Blade Balancing Test Stand (figure 1). The facility is used mainly for production dynamic and aerodynamic balancing of main rotor blades in order to insure blade interchangeability.

The traverse mechanism and pressure scanning valve were mounted in the tip cap of a CH-53A rotor blade specially modified for this test. The blade, illustrated in figure 2, has a tip radius when mounted of 11 m (36.12 ft) and a chord of 0.67m (26.0 in.). The airfoil section is a modified NACA 0011 profile. Blade construction is conventional with aluminium D spar and fabricated sheet metal pockets. The outer 2.5% of the blade is a hollow, detachable tip cap. The units to be whirled were mounted inside the tip cap (figure 3). They were attached to a bar (figure 4), which was clamped in turn to the studs that would, in normal operation, carry the tip weights. The whole assembly was then adjusted to the same balance condition as the basic blade by adding extra weights.

Instrumentation wiring was led out of the tip cap to a contact strip on the blade lower surface near the tip (figure 4). The leads were bonded to the spar, close to the blade elastic axis, and carried to a terminal block at the root. With the exception of the hot wire anemometer cables the leads were then plugged into the test stand slip ring assembly and fed into the stationary system. In the interest of maintaining good signal to noise characteristics the hot wire anemometer amplifiers were mounted in the rotating system on a platform over the shaft axis (figure 5). After amplification the high level signal was taken out through the slip rings for further treatment in the control room.

TRAVERSE DESIGN

The principal design aim of the traverse mechanism was to provide the capability to obtain good quality boundary layer data in a centrifugal acceleration field of up to 400 g while maintaining control over placement of the measureing device, hot wire or pitot probe, to the levels possible in a non rotating environment. A traverse distance of 2.5 cm (1.0 in.) with positioning accuracy of at least 0.0025 mm (0.0001 in.) were set as goals. In order to minimize extra centrifugal loads on the test blade a weight of 0.45 kg (1.0 lb) was taken as the maximum acceptable. The size has to be small enough to allow mounting within the nominally 11% thick, 0.66m (26.0 in.) chord airfoils of CH-53 rotors and permit measurements of boundary layer development from within 10% to at least 80%, and preferrably 95%, of chord. This constrained the maximum traverse depth to not more than 2.5 cm (1.0 in.).

On the basis of experience with actuators in both model and full scale rotating machinery the worm gear/worm wheel system was chosen. The schematic in figure 6 illustrates the principle. An electric motor turns the worm gear train. The center of the worm wheel is threaded and with the probe stem constrained from rotating the rotary input motion emerges as a linear output. The sensitivity of the system is determined by the gear ratio chosen and by the pitch of the screw on the probe stem. If the drive is provided by a stepper motor then controllability and sensitivity of the system is further enhanced. The sensitivity of the present prototype system was determined by the gears and stepper motors which were readily available. A stepper motor with twenty four 15 degree steps, driving a 60 tooth, 48 pitch worm wheel through the appropriate worm gear and an 18 TPI (threads per inch) probe stem results in 1 mm of probe displacement for every 1000 pulses supplied to the motor. The traverse case was machined out of aluminium alloy with the gears and probe stem running in steel bushing inserts. Final weight of the fully assembled traverse and probe was 0.29 kg (0.65 lb).

INSTRUMENTATION

Chordwise and spanwise velocity components were measured using a two element hot wire anemometer probe with the wires arranged in a V parallel to the local surface, figure 7. The wires were $5\mu (5 \times 10^{-6}m)$ platinum plated tungsten wires, with an active length of 2mm, set at an angle of ±45 degrees to the chordline. Conventional constant temperature units were used with the amplifiers mounted in the rotating system. After passing through the slip ring assembly the anemometer output was linearized in the fixed system. A schematic of the instrumentation is given in figure 8.

Power for the stepper motor is supplied by a low voltage power supply, pulse source and controller. Motor and hence traverse speed is determined by the pulse frequency and direction of motion by the polarity of the wave train. Probe position is found by simply counting the number of pulses supplied as the traverse proceeds from a known datum. Because of the exploratory nature of the experiment and lack of knowledge of the stepper motor behavior in a centrifugal field a back up position sensing device was employed. A multi-turn helical potentiometer was driven from the worm gear, at the end opposite the stepper motor input, through a pair of spur gears and a 108 : 1 reduction gearbox. This gave a direct mechanical connection between the probe and the position sensing device, one which would not be susceptible to the slipping or "slewing" of the magnetic coupling in the stepper rotor if it stalled under load.

A commercially available miniature pressure scanning valve, together with a standard diaphragm pressure transducer were tested for whirl compatability during traverse testing. The unit was clamped to the traverse mounting beam with its axis in a chordwise direction to minimize the effects of centrifugal accelerations. The scanning valve was designed to accept up to 36 separate pressure inputs and was driven from a constant voltage DC power supply. An integral encoder gave a port position output, displayed in binary form, and an indication when the scanning switch passed the "home" position.

DEMONSTRATION OF FEASIBILITY

Testing was broken into two main phases. They were the demonstration of the whirl compatability of the traverse mechanism and the pressure scanning system and the measurement of the boundary layer characteristics on the tip of the test blade.

The probe was set at the outer limit of its travel 2.5 cm (1 in.) above the surface and the rotor taken up to maximum speed, 185 RPM. Having demonstrated that the assembly held together over the centrifugal load range and the instrumentation system was operating satisfactorily the rotor was slowed and stopped.

The probe was then retracted until it was just above the surface and its position checked. This was taken as the datum position and the pulse counter zeroed. The rotor speed was then set at 50 RPM and the traverse run out to the limit of its travel, and in again, several times. During traversing primary and secondary probe position outputs, pulse count and potentiometer voltage respectively, were recorded together with pressure scanning valve drive motor current, scanning rate and pressure transducer output. The process was repeated at 100, 125, 150 and 175 RPM.

Above 125 RPM it was noted that the stepper motor was "slewing" under the heavy centrifugal load. This meant that, although the motor could still drive the traverse, the pulse count, because of the failure of the motor to respond to every pulse, could not be used as a reliable indication of position. The slippage became progressively worse as the rotor speed was increased until at 175 RPM the stepper motor could barely move the traverse. The secondary position sensing device was insensitive to centrifugal load with no drift as rotor speed was increased to the maximum.

At each rotor speed the pressure switch was scanned several times. There was no perceptible change in either scanning rate or motor current drain over the full rotor speed range. Similarly, no change was noted in the output of the pressure transducer indicating insensitivity to centrifugal effects.

Having explored the effective range of the present device the boundary layer velocity profiles were measured at 50, 125 and 175 RPM at rotor collective pitch settings of 1 and 5 degrees. For the two low speed cases the probe was traversed with the rotor speed being maintained. At 175 RPM the rotor was slowed between data points to speed up the traversing. Because of the very sudden leading edge separation, with no trailing edge flow breakdown, that characterizes stall on the NACA 0011 (MOD) airfoil section of the blade used, it was not possible to investigate the nature of separated flows in the rotating system.

DATA REDUCTION

The linearized hot wire output voltages were converted to velocities using the free air calibrations given in figure 9. Where appropriate the velocities were corrected for wall proximity effects following reference 15. In this test the wall correction was very minor since it only becomes significant in the laminar region close to the surface. Probe position was found from the dual pulse count, potentiometer position calibration given in figure 10.

The variation of wire cooling velocity, the mean velocity perpendicular to the wire axis, is plotted as a function of distance above the surface in figure 11 for rotor speeds of 125 and 175 RPM and collective pitch settings of 1 and 5 degrees. Because the wires are set at $\pm$ 45 degrees to the chordline calculation of the chordwise and spanwise velocity components from the cooling velocities is a simple matter. If C_1 and C_2 are the cooling velocities from wires 1 and 2 respectively, then the chordwise and spanwise velocities are given, to the first order, by

$$u = \frac{C_1 + C_2}{\sqrt{2}} \qquad + \quad \text{towards the trailing edge}$$

$$v = \frac{C_1 - C_2}{\sqrt{2}} \qquad + \quad \text{outwards from axis}$$

The chordwise and spanwise velocity profiles are given in dimensional form in figure 12 and non dimensionalized by boundary layer thickness and free stream chordwise velocity in figure 13. Because of the irregular nature of the profiles and the exploratory nature of the program no further treatment of the data is presented.

DISCUSSION

Figure 14 presents a summary of the range of conditions over which the traverse and pressure scanning valve were tested and identifies the conditions at which boundary layer data was obtained. The traverse mechanism as designed operated with complete success up to 125 RPM, a centrifugal acceleration of 188g. That is, the probe was traversed over the full range and its position was tracked using the primary, pulse count, method. Between 125 RPM and 175 RPM, or up to 366g centrifugal acceleration, the probe could be traversed, only very slowly at 175 RPM, but the position could not be tracked using the primary method. The secondary method did however operate successfully. Above 175 RPM the stepper motor could not move the probe. The structural integrity of the system was however demonstrated up to the maximum attainable speed of 185 RPM, 410g centrifugal acceleration, with the probe both retracted and fully extended. No damage was sustained either by the traverse mechanism or the hot wire elements at the extreme condition. This represents a local Mach number in excess of 0.65.

One reason for the failure of the traverse to meet its design goal of operation at 400g is felt to be higher than anticipated bearing loads between the worm wheel and the upper and lower bearing surfaces. This is indicated as a probable cause by the difference noted in the power required to drive the probe up as opposed to down. As the worm gear turns, the worm wheel tends to ride up or down on the helix depending on the direction of rotation. This will be aggravated by any deflection of the wheel caused by the centrifugal effects. The upper bearing face is considerably larger than the lower with correspondingly increased friction torque. The use of miniature ball or roller bearings in future developed versions of the traverse, instead of the present journal bearings, and an associated marked reduction in friction, will expand the operating range. The principal factor leading to the failure to meet specification however was felt to be the inclusion of the secondary position sensing system. The spur gears, reduction gear train and potentiometer inevitably reduce the share of motor torque available for the traverse. Since developed versions of the mechanism will not have this secondary system there is little doubt that the design goal of 400g will be achieved.

There is little that can be said about the operation of the pressure scanning switch other than that it operated successfully over the whole rotor speed range. This device expands the capability to make pressure measurements in the rotating system. Particularly, it should upgrade considerably the precision of blade surface pressure measurements since it allows the pressure to be sensed over a wide area with one high quality transducer rather than the large number of individual units currently employed. It offers too, a considerable simplification in the amount of wiring that has to be carried on the blade and a considerable reduction in the slip ring capacity required. There is a penalty which must be payed however. The frequency response of the switching system will inevitably be restricted by the length of tubing between the pressure tap and the transducer. It should nevertheless be possible to maintain responses of the order of 2 times the rotational frequency for typical helicopter main rotors by careful positioning of the scanning unit and adjustment of tube lengths.

The boundary layer velocity profiles, figures 11 through 13, show traces of the environment in which they were measured and are far from the profiles which would be expected in the ideal case. Special preparation of the blade surface was beyond the scope of the present program. Consequently, some distortion of the measured velocity profiles can be expected as a result of the surface irregularities present. Inspection of figure 3 shows four potential sources of interference. They are, the joint between the leading edge abrasion strip and the surface, a screw hole in front of and slightly outboard of the survey location, the tip light fairing and a slight surface ripple which appears when the tip cap retaining screws, absent in figure 3, are inserted and tightened down. Influence of the tip light and the surface ripple will be small. The light, although large, is outboard and well removed from the survey location and the wavelength of the surface ripple is large when compared with the boundary layer thickness. The form of the irregularity in the velocity profile, a reduction in the chordwise velocity in the outer region, points toward the abrasion strip joint as being the most likely cause. The profiles are typical of those measured behind a discrete transition element such as a wire or a downstream facing step. The single screw hole was filled with wax and well smoothed down and is not felt to be a significant factor.

Despite all these sources of potential interference the overall form of the three dimensional boundary layer is evident. The chordwise velocity profile presented in figure 15 is close to that predicted using reference 10. The theoretical boundary layer growth was calculated using the local measured free stream velocity and a pressure distribution based on an estimated local blade angle of attack. The measured and calculated boundary layer thickness (defined as the distance above the surface where the chordwise velocity ratio equals 0.995) were 0.0567mm and 0.0591mm respectively, good agreement when the assumptions inherent in the theory are considered. Because of the irregularities in the measured profiles no attempt was made to calculate the characteristic boundary layer momentum and displacement thicknesses. The measuring station is aft of the blade quarter chord line, and consequently the axis of rotation, and in the absence of any tip vortex effects the radial flow should be inwards. This inward flow can be seen on all the cases presented.

Although the data presented here are not of very high quality the test has demonstrated that it is possible to make measurements in a rotating system using a traversed hot wire anemometer. Improvements in the quality of the data will come with the further exercise of the technique and, particularly important, when the surface over which the boundary layer is growing is specially prepared. Based on the tests reported here there appears to be no reason why it should not now be possible to obtain information on the behavior of boundary layers in a rotating system of a quality equivalent to that obtainable in a non rotating environment.

CONCLUSIONS

From the tests carried out and described above the following conclusions may be drawn.

(1) The traverse mechanism developed under this contract will operate effectively in the 400g centrifugal accelerations commonly met in the helicopter rotor environment.

(2) Pressure scanning switch equipment is available commercially which will allow the measurement of many rotor blade surface pressures with one high quality pressure transducer in centrifugal accelerations in excess of 400g.

(3) Conventional hot wire anemometer equipment can be used for rotor blade boundary layer measurements, in the open air, at full rotor tip speeds without any special precautions being taken.

With these conclusions the principal objectives of the program were met.

RECOMMENDATIONS

With the feasibility of rotor blade boundary layer measurements demonstrated this type of equipment should be used to explore the following areas where information is urgently needed to complement analytical studies.

(1) Evaluation of the effects of centrifugal and Coriolis accelerations on boundary layer development.

(2) Detailed exploration of the influence of centrifugal and Coriolis accelerations on the mechanism of turbulence.

(3) Study of the influence of the effects of rotation on laminar separation, particularly the behavior of laminar separation bubbles.

(4) Study of the effects of rotation on boundary layer separation (and eventually on airfoil $C_{L\ max}$ and stall).

(5) Investigation of the effects of rotation on the unsteady boundary layer - the helicopter rotor in forward flight.

(6) Exploration of the formative tip vortex and general rotor blade flow field studies.

Having developed a compact, rugged, traverse mechanism, applications need not be limited to the helicopter rotor and many other uses are foreseen. Most promising is in the field of unsteady aerodynamics where the traverse is small enough to be mounted inside oscillating surfaces and provide detailed survey capability in the surrounding flow.

Sikorsky Division
United Aircraft Corporation
Stratford, Connecticut November 30, 1972

REFERENCES

1. Kuethe, A. M.; McKee, P.B.and Curry, W. H.: Measurements in the Boundary Layer of a Yawed Wing. NACA TN 1946, 1949.

2. von Karman,T.: Uber Laminare and Turbulente Reibung, ZAMM, Vol. 1, 1921 pp. 233.

3. Cham, T-S and Head, M. R.: Turbulent Boundary Layer Flow on a Rotating Disc. J. Fluid Mech., Vol. 37, part 1, 1969, pp. 129 - 147.

4. Lakshminarayana, B.; Jabbari, A. and Yamaoka, H.: Turbulent Boundary Layer on a Rotating Helical Blade. J. Fluid Mech., Vol. 51, part 3, 1972, pp. 545-570.

5. Fogarty, L. E.: The Laminar Boundary Layer on a Rotating Blade. J. Aeron. Sci., Vol. 18, No. 4, 1951, pp 247-252.

6. Mager, A.: Generalization of Boundary Layer Momentum-Integral Equations to Three-dimensional Flows including those of Rotating Systems. NACA Rept. 1067, 1952 (supersedes NACA TN 2310).

7. McCroskey, W. J. and Yaggy, P. F.: Laminar Boundary Layer on Helicopter Rotors in Forward Flight. Preprint 68-70, American Institute of Aeronautics and Astronautics, January 1968.

8. McCroskey, W. J. and Dwyer, H. A.: Methods of Analyzing Propeller and Rotor Boundary Layers with Crossflow. Proceedings of the NASA Symposium on Analytic Methods in Aircraft Aerodynamics, NASA SP-228, 1969, pp. 473-514.

9. McCroskey, W. J.; Nash, J. F. and Hicks, J. G.: Turbulent Boundary Layer Flow over a Rotating Flat Plate Blade. J. AIAA, Vol. 9, No. 1, 1971 pp 188-189.

10. Clark, D. R. and Arnoldi, D. R.: Rotor Blade Boundary Layer Calculation Programs. USAAVLABS Technical Report 71-1, March 1971.

11. Tanner, W. H. and Wohlfeld, R. M.: New Experimental Techniques in Rotorcraft Aerodynamics and their Application. J. AHS, Vol. 15, No. 2, April 1970.

12. Tanner, W. H. and Buettiker, P.: The Boundary Layer of the Hovering Rotor. Paper presented to the joint CAL/USAAVLABS Symposium on the Aerodynamic Problems of V/STOL Aircraft, Vol. III, Aerodynamic Research on Boundary Layers, June 1966.

13. McCroskey, W. J. and Durbin, E. J.: Flow Angle and Shear Stress Measurements using Heated Films and Wires. ASME Trans. Series D, J. Basic Engrg, Vol. 94, No. 1, pp. 46-52, March 1972.

14. Blaser, D. A. and Velkoff, H. R.: Boundary Layer Velocity Profiles on a Helicopter Rotor Blade in Hovering and Forward Flight. Preprint No. 622, American Helicopter Society 28 Annual National Forum, May 1971.

15. Oka, S. and Kostic, Z.: Influence of Wall Proximity on Hot Wire Velocity Measurements. Information Report No. 13, DISA Electronics, Franklin Lakes, N. J., May 1972.

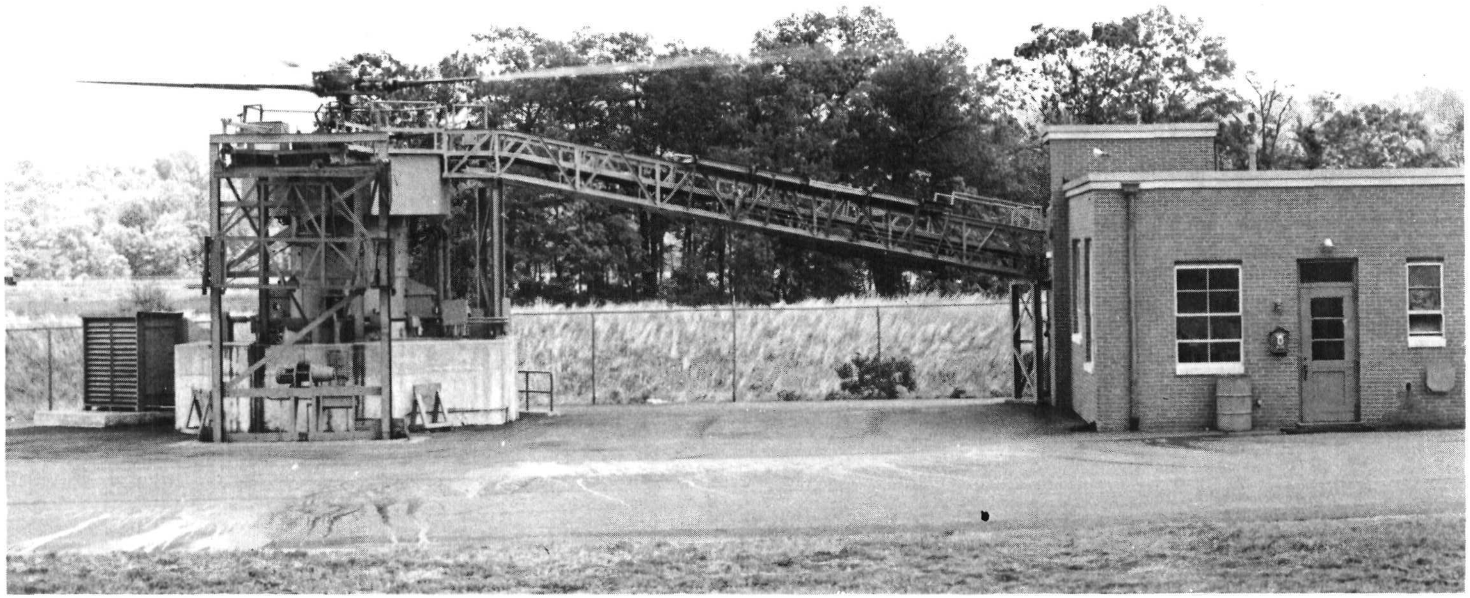

Figure 1. Sikorsky Blade Balance Stand

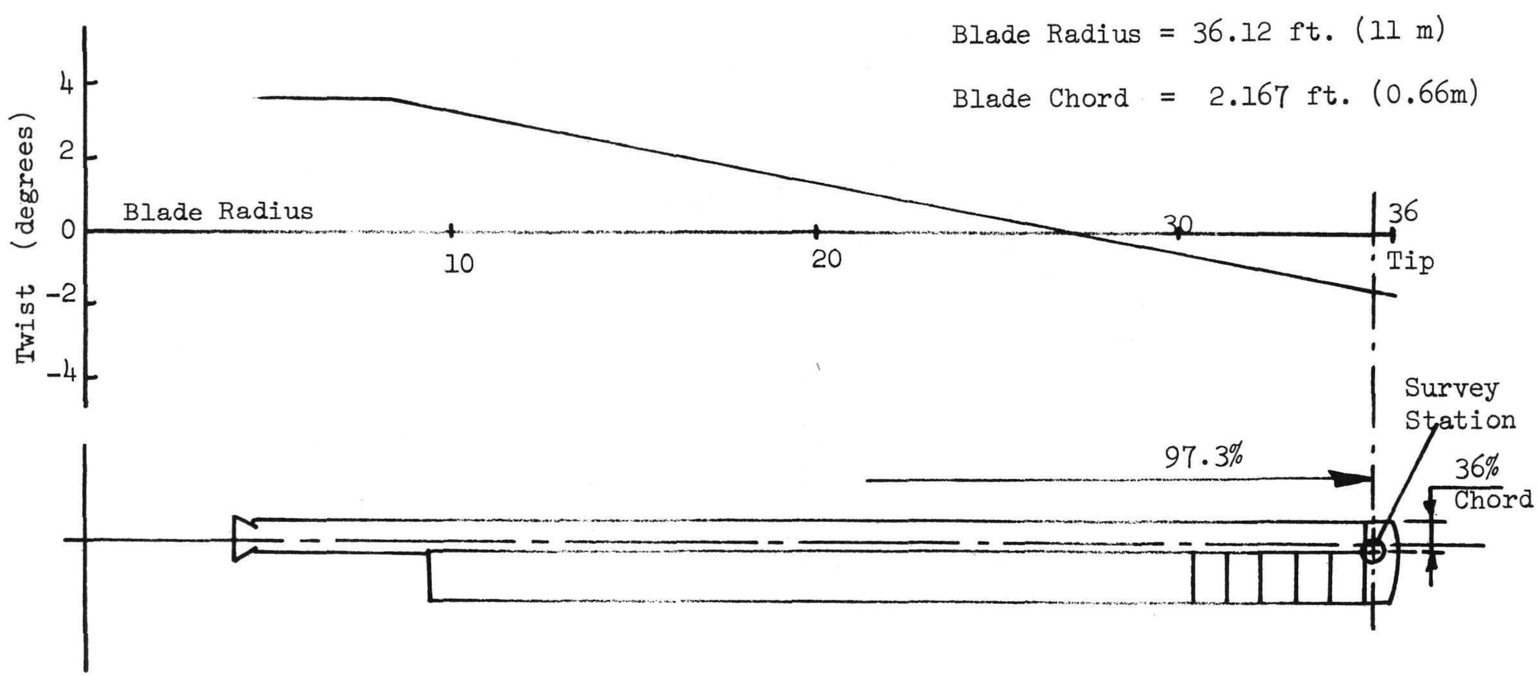

Figure 2. CH-53A Main Rotor Blade Schematic.

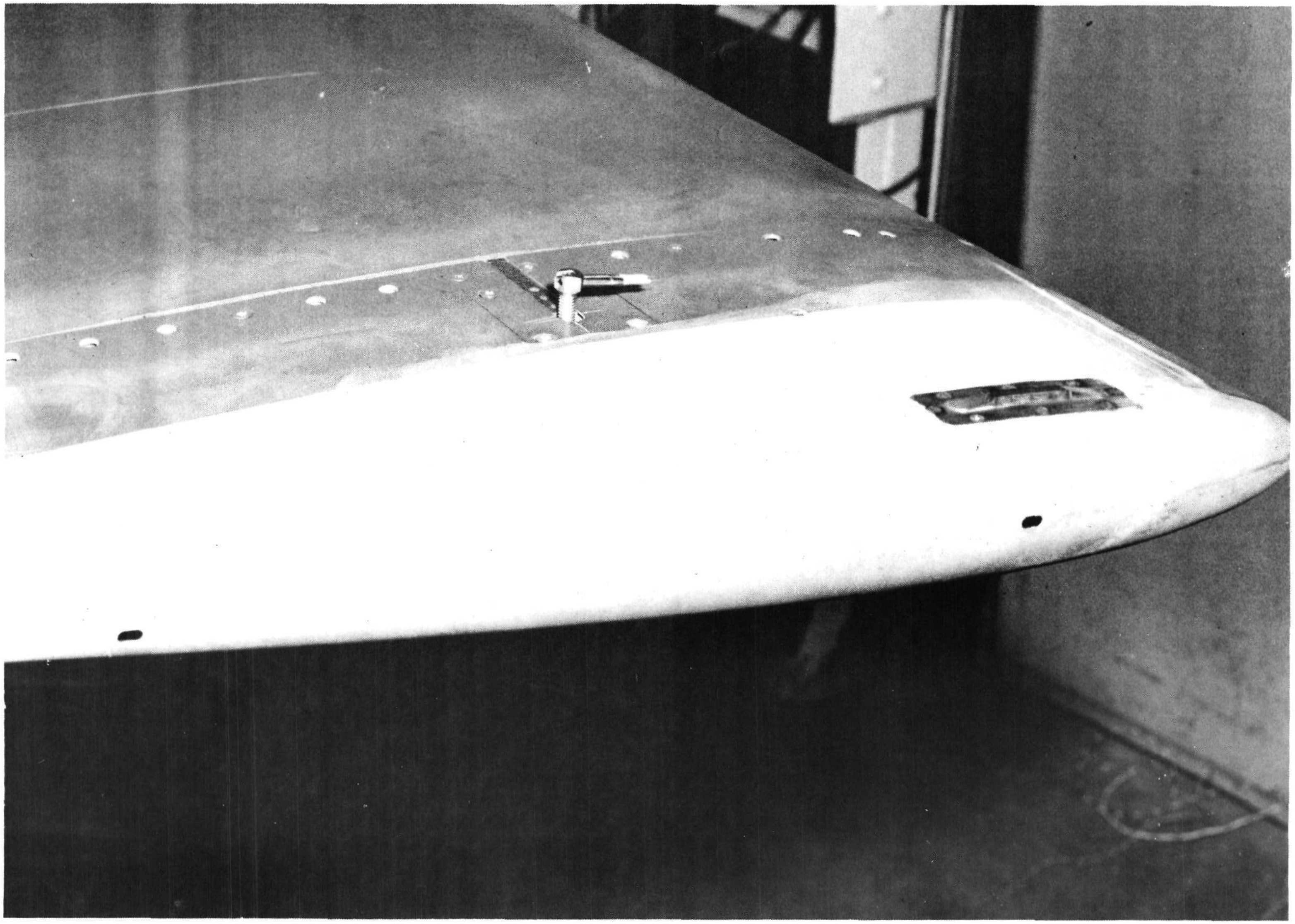

Figure 3. Tip cap with traverse installed.

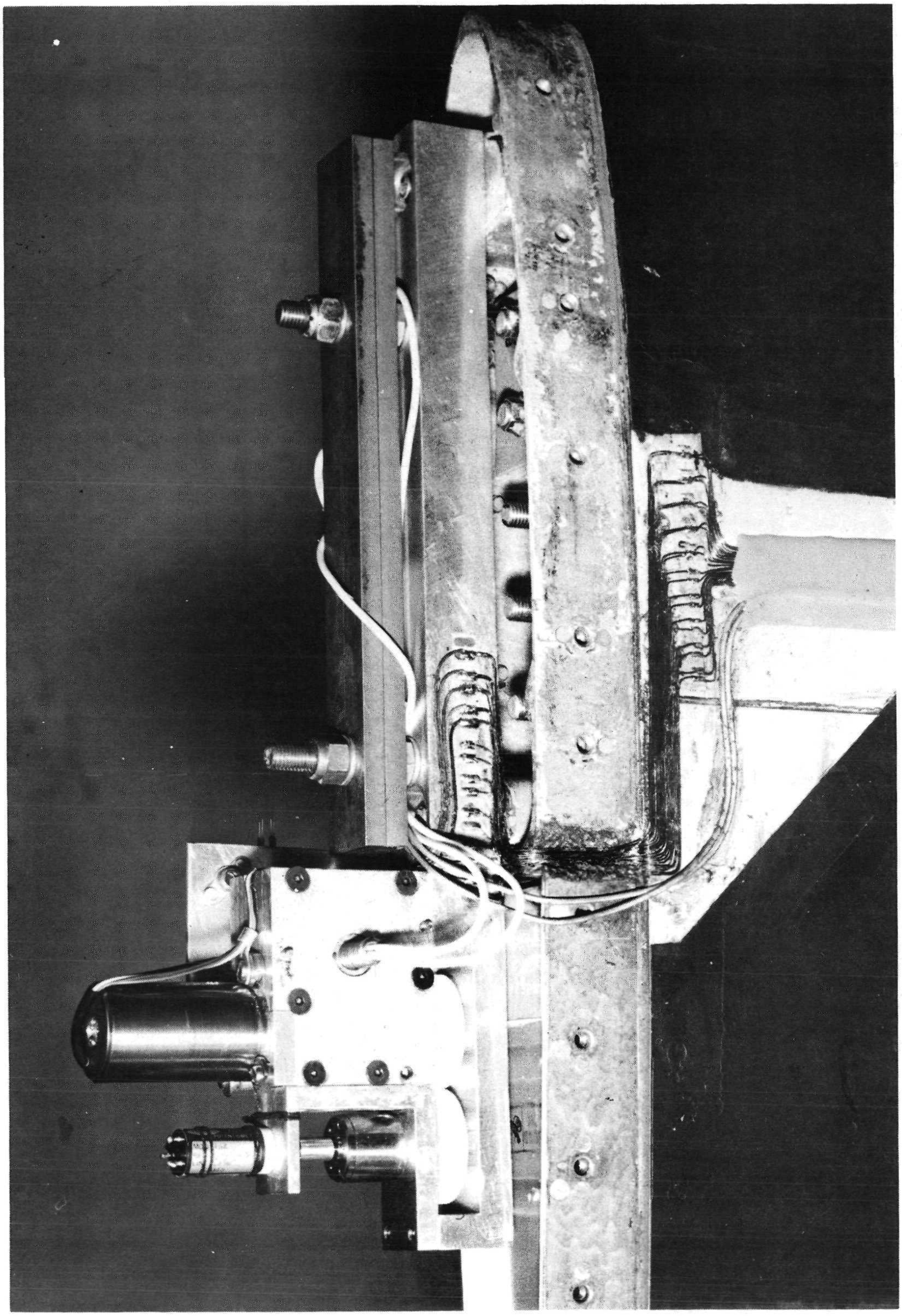

Figure 4. Traverse Installation

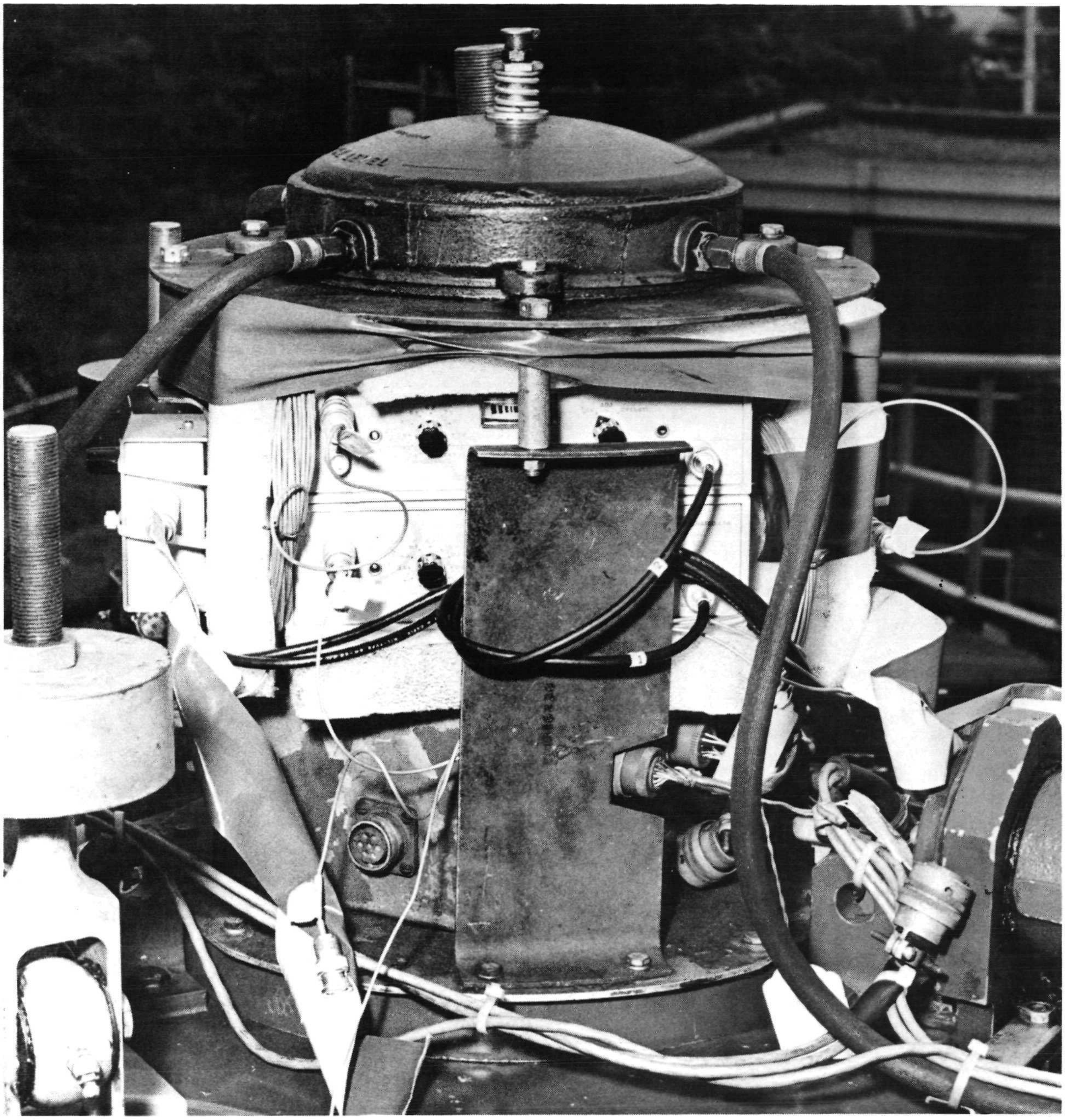

Figure 5. Anemometer installation in rotating system.

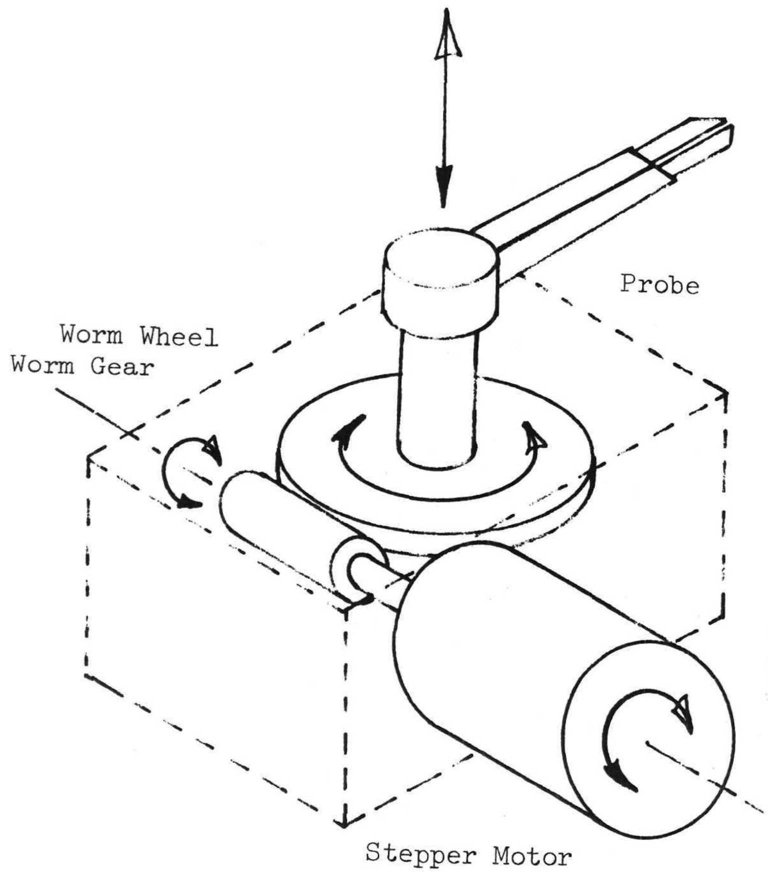

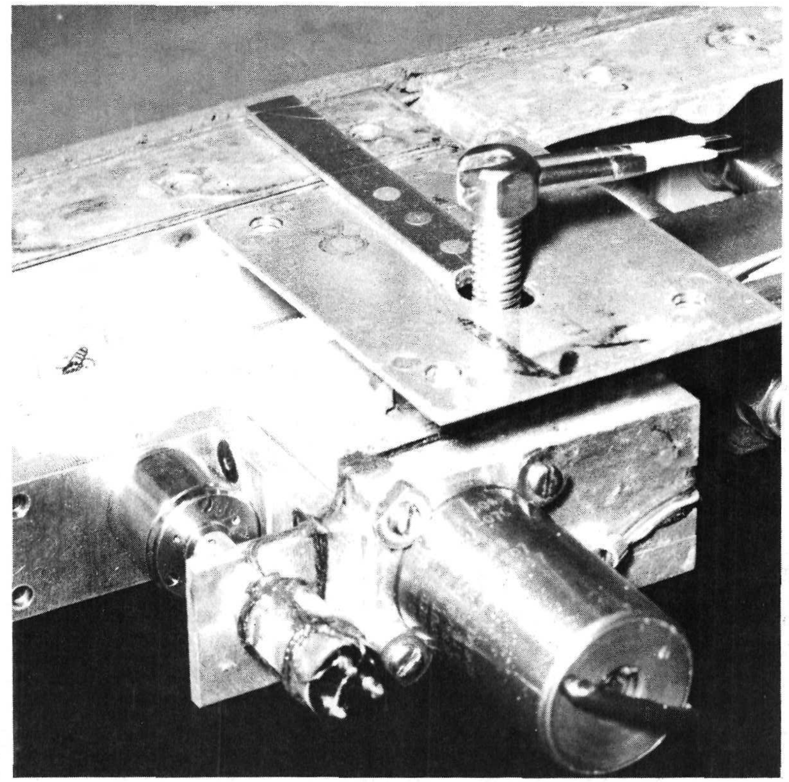

Figure 6. Traverse Mechanism.

SCALE: Approx 2 x Full Size

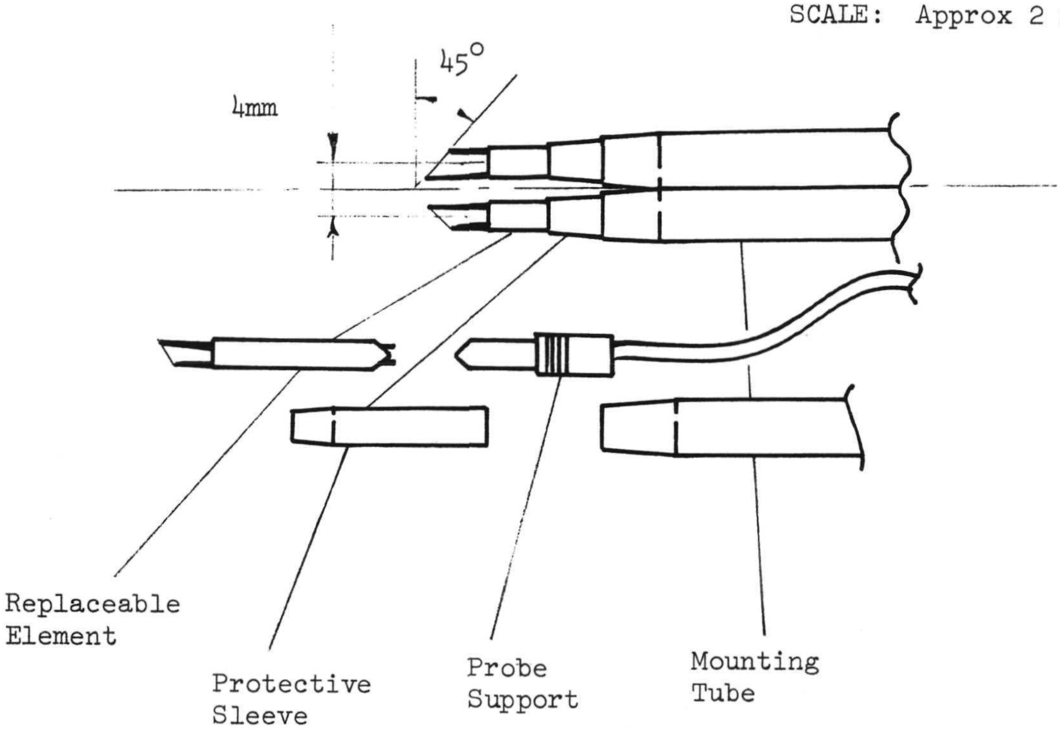

Figure 7. SCHEMATIC OF HOT WIRE PROBE UNIT

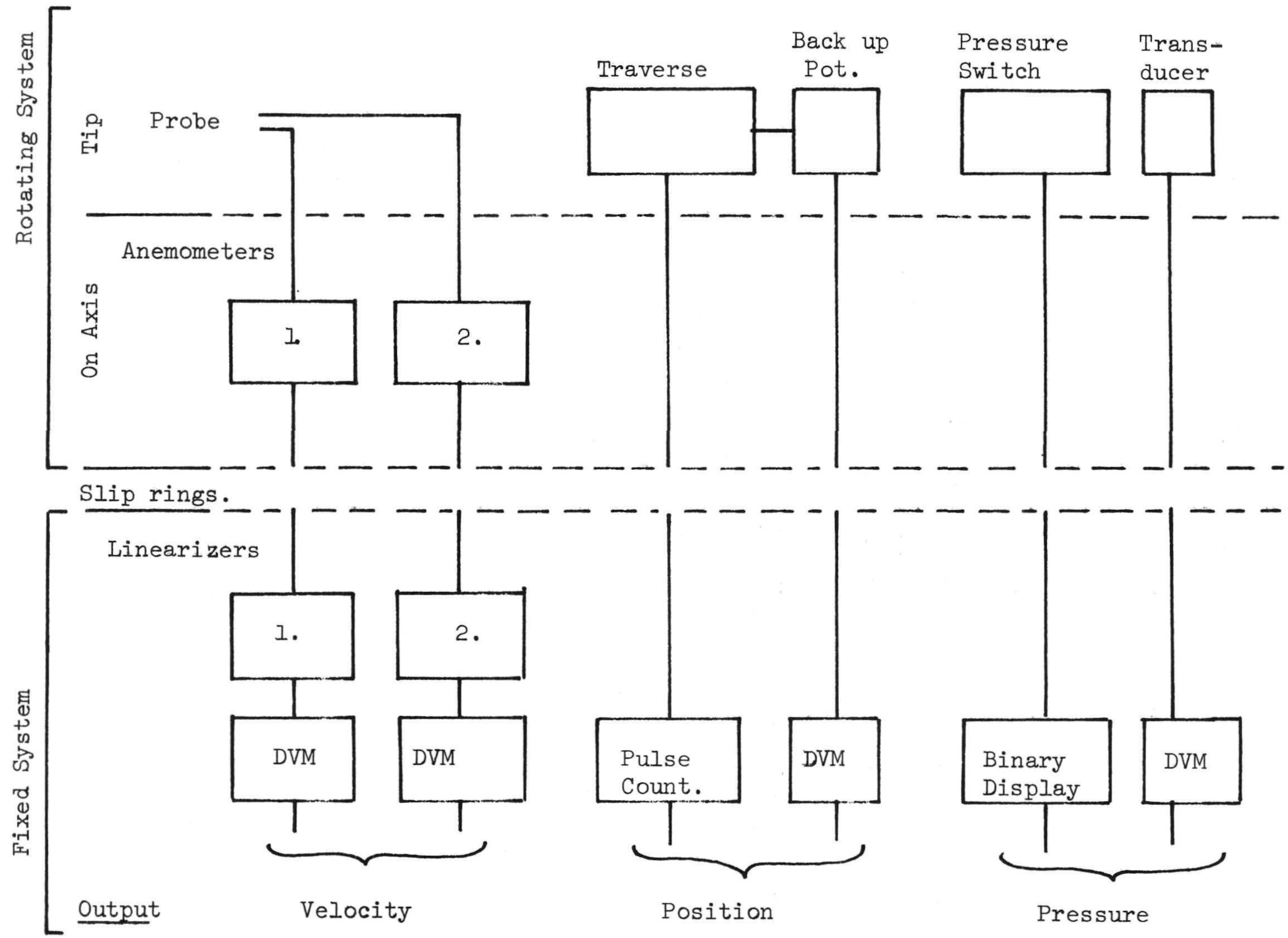

Figure 8. Instrumentation Schematic.

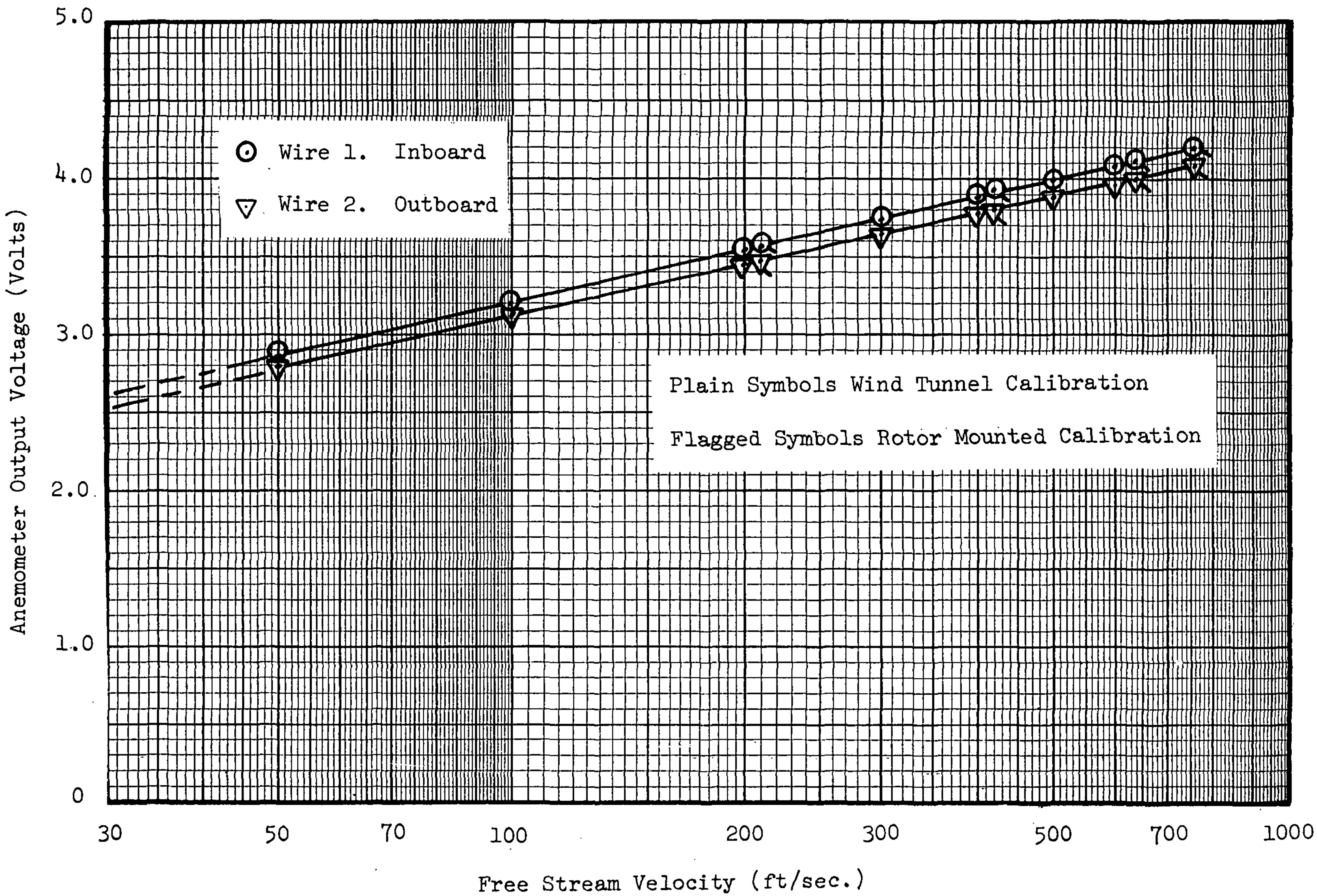

Figure 9. Hot Wire Anemometer Calibration

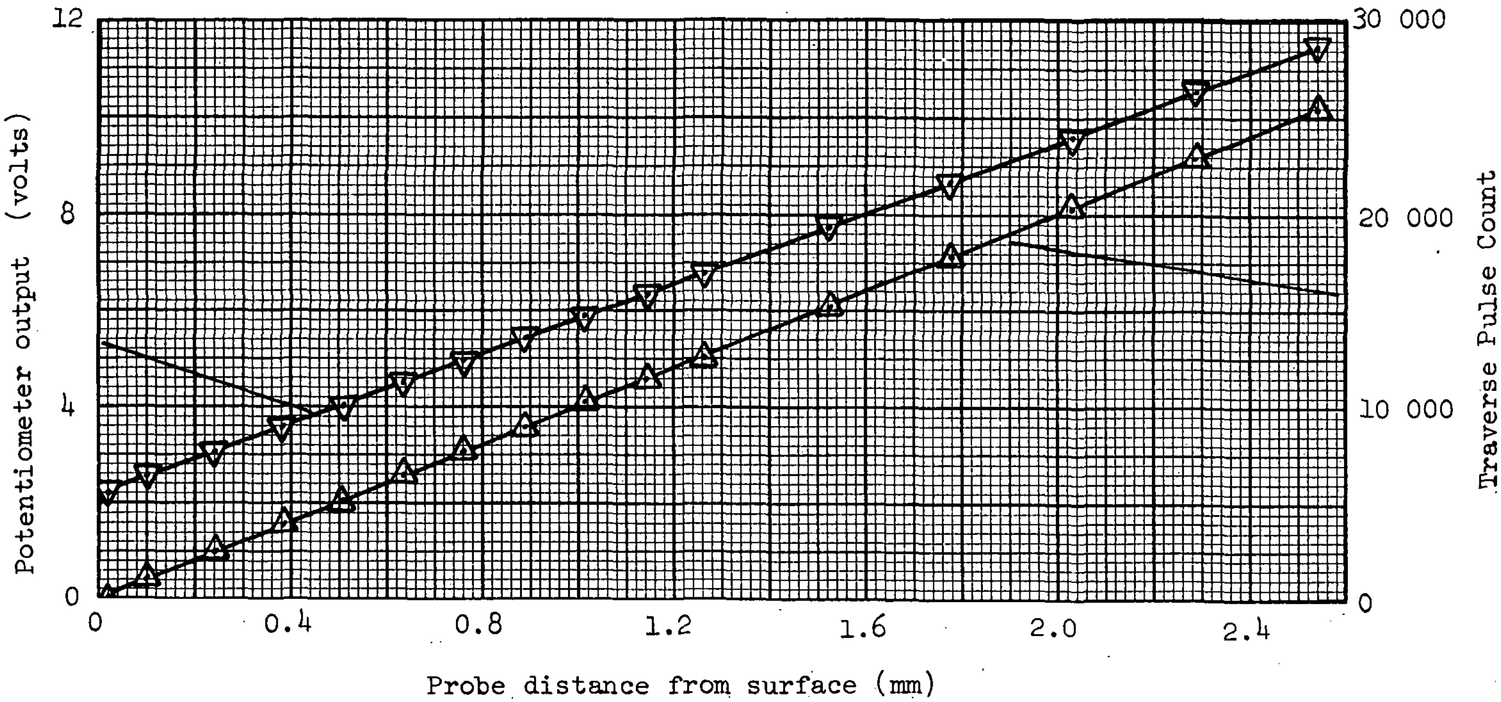

Figure 10. Traverse Calibration

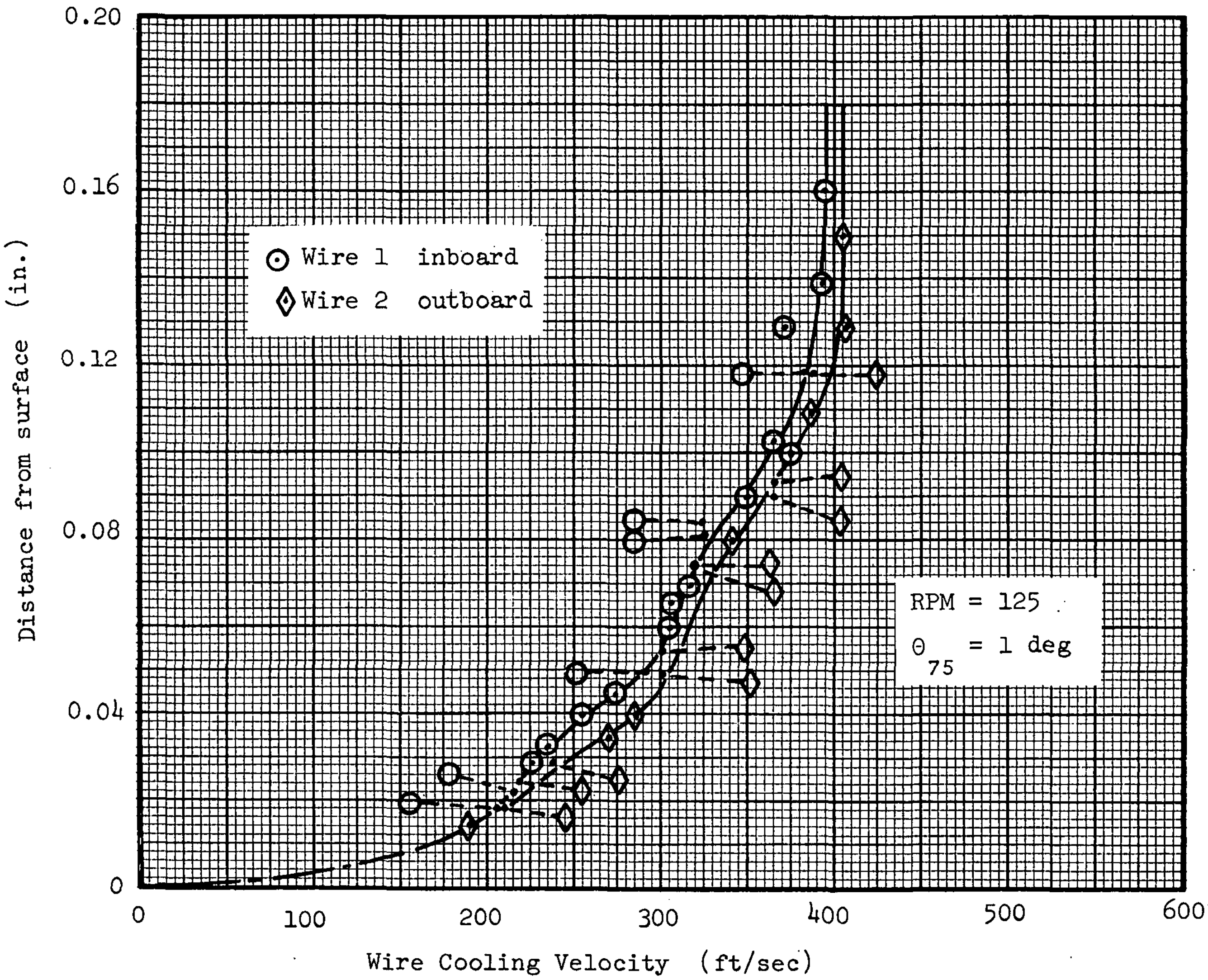

Figure 11. Typical Cooling Velocity Distributions

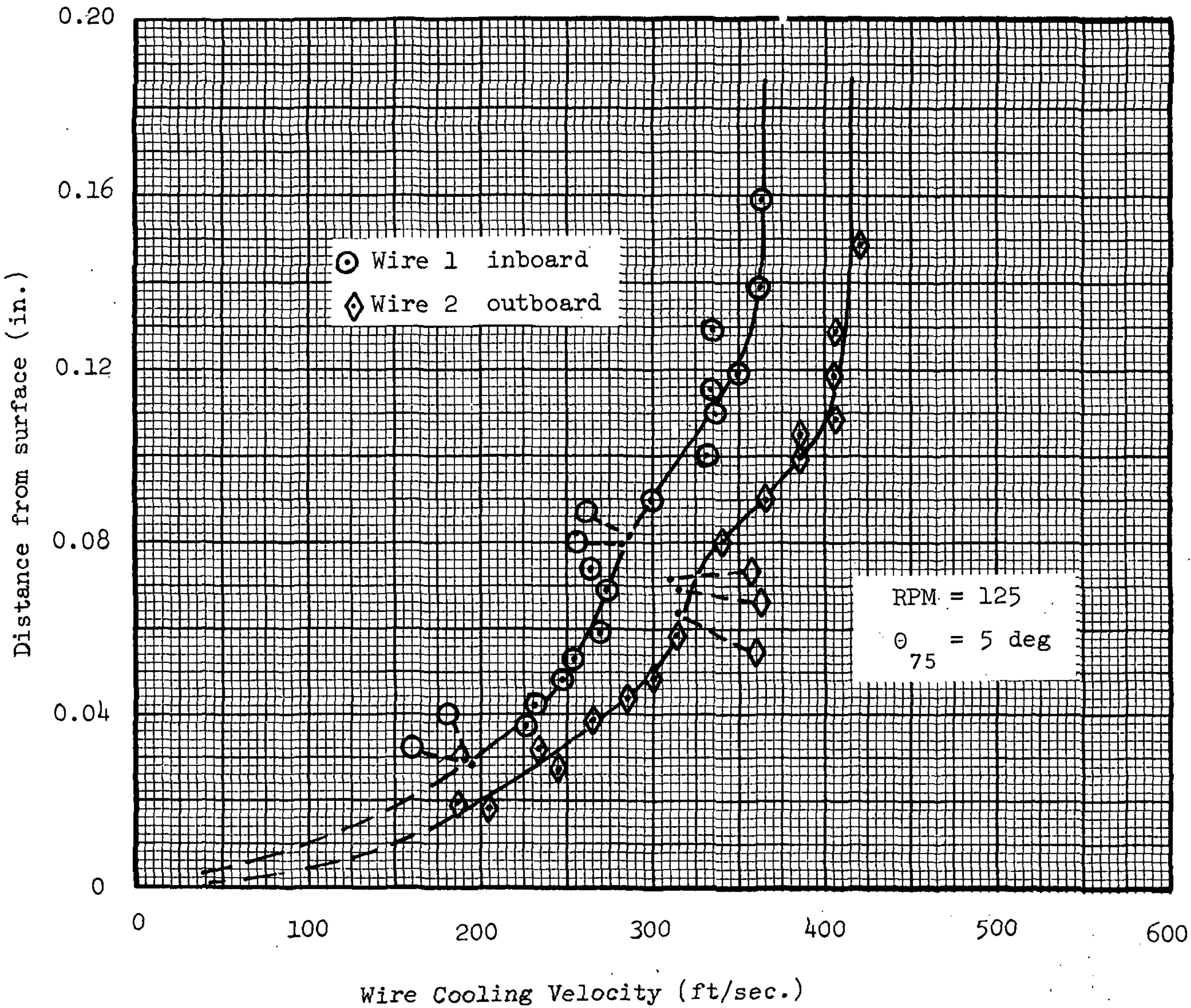

Figure 11. continued

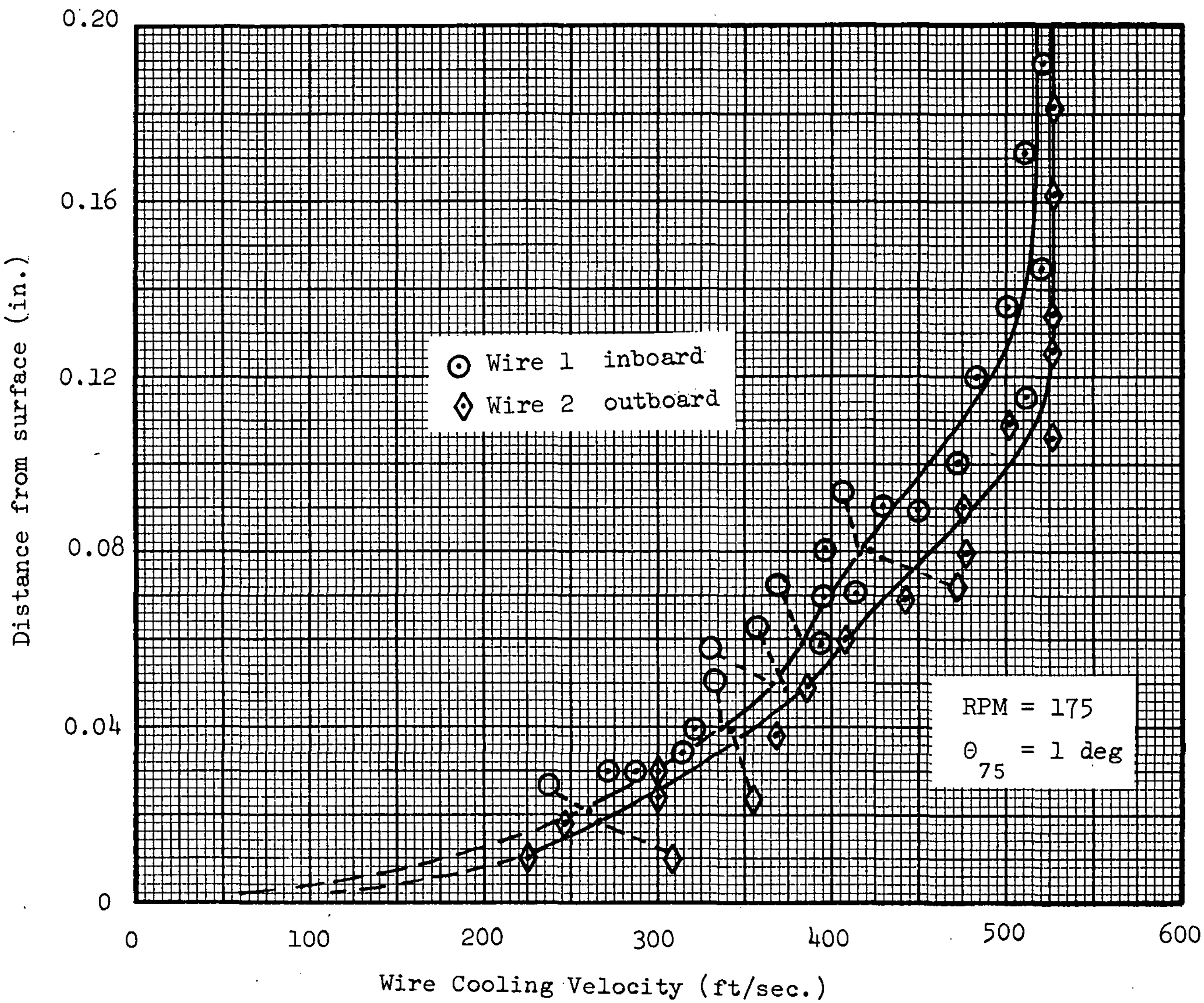

Figure 11. continued

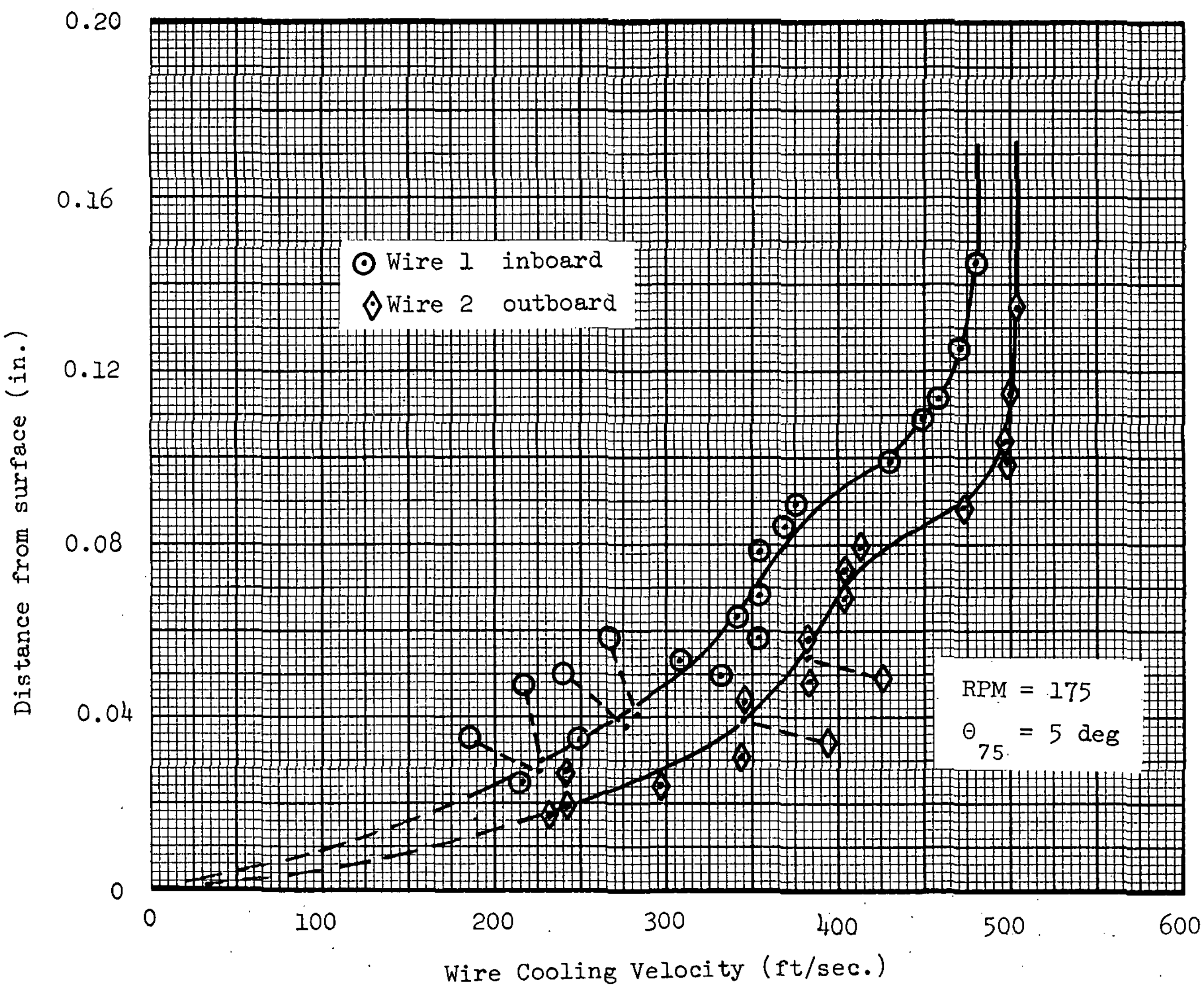

Figure 11. concluded.

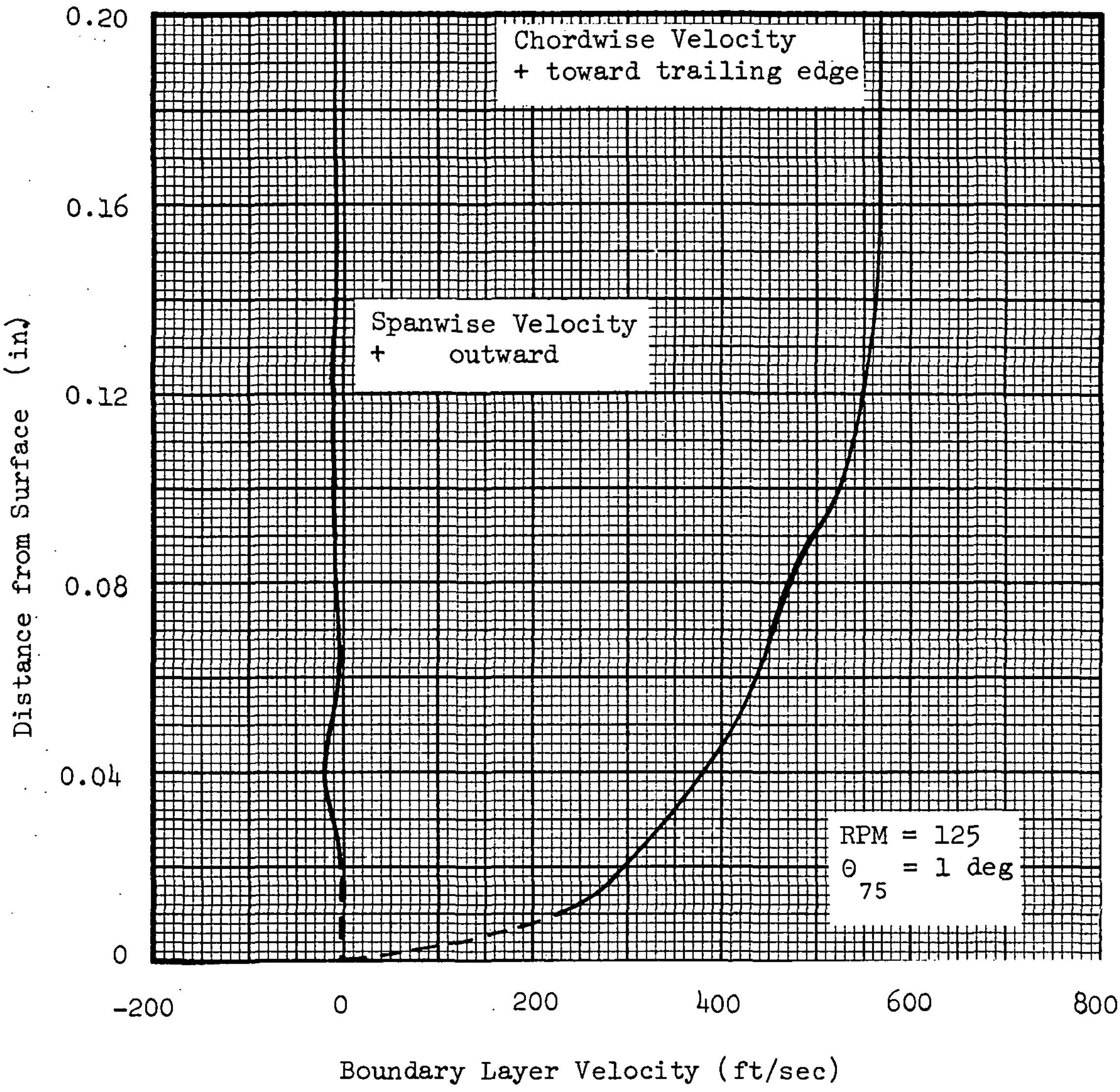

Figure 12. Typical Chordwise and Spanwise Velocity Profiles

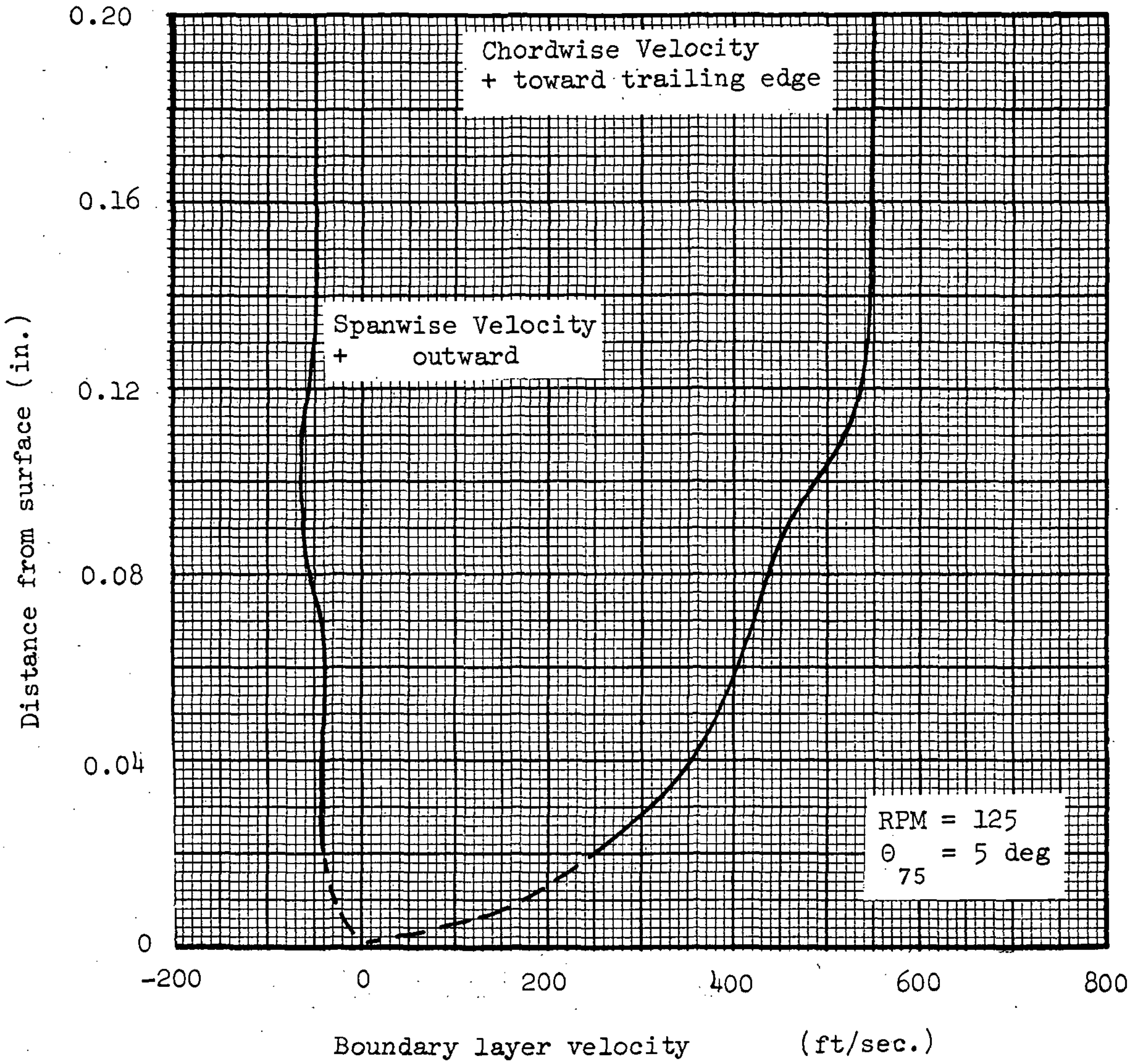

Figure 12. continued

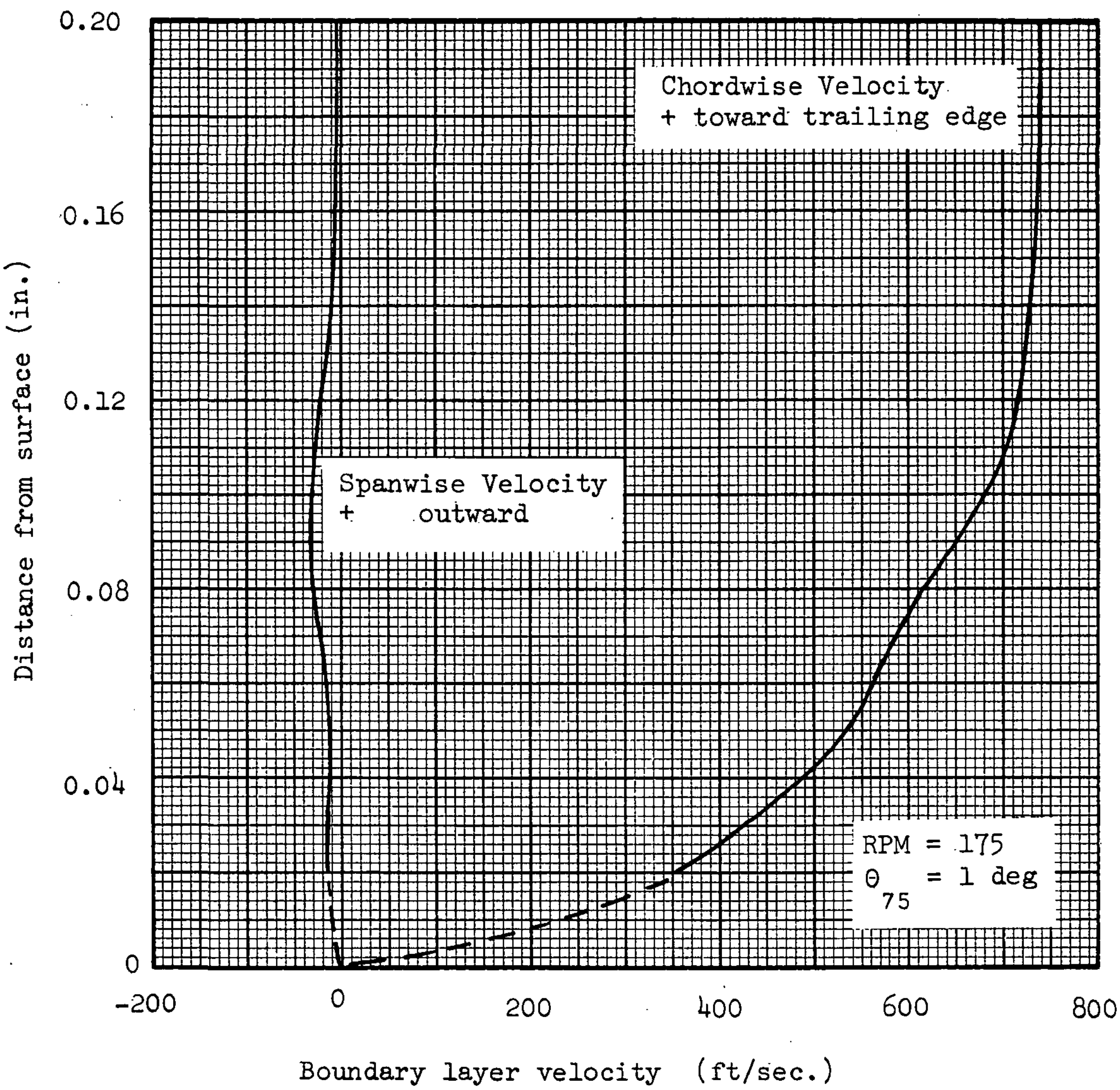

Figure 12. continued

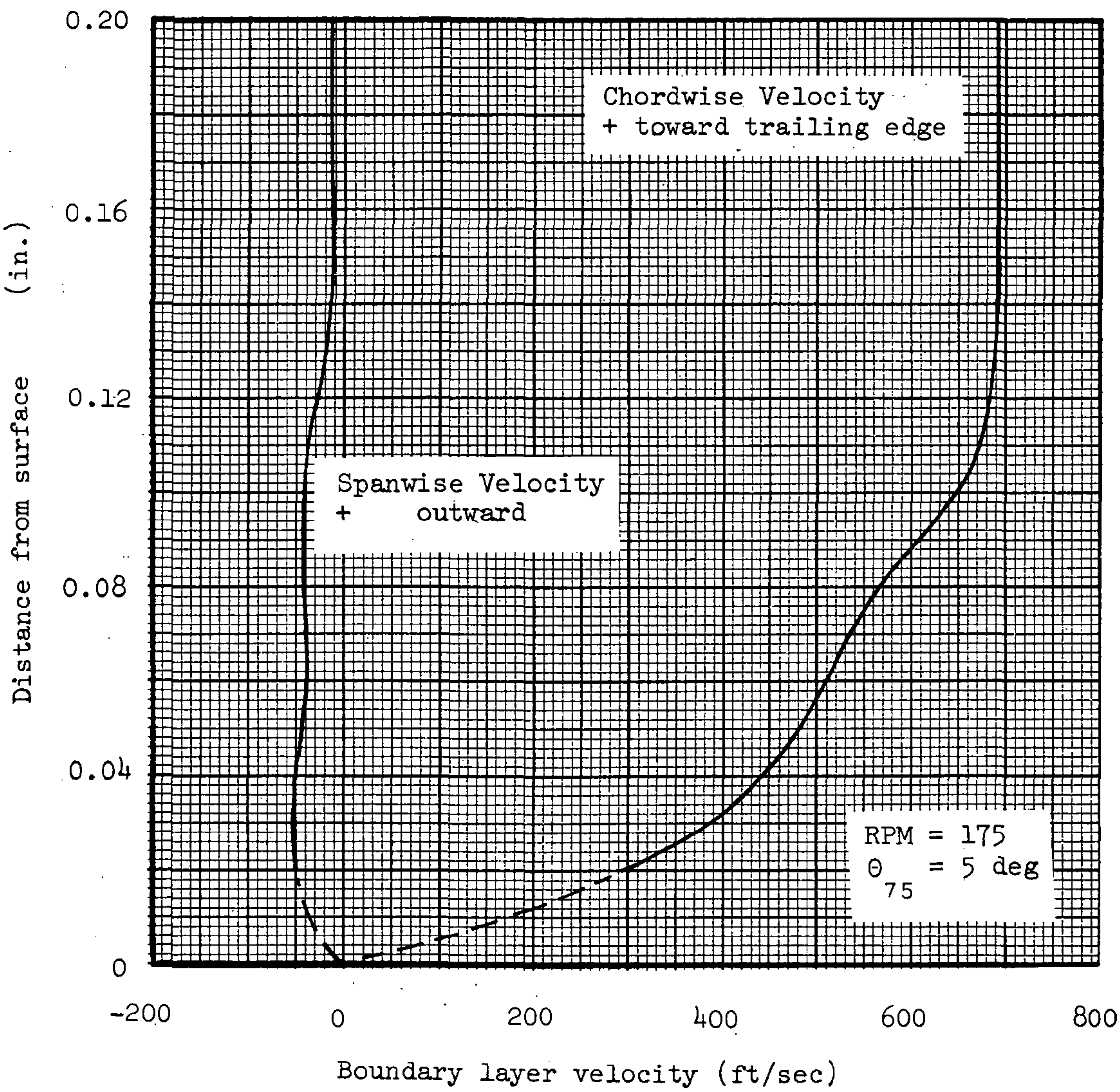

Figure 12. concluded.

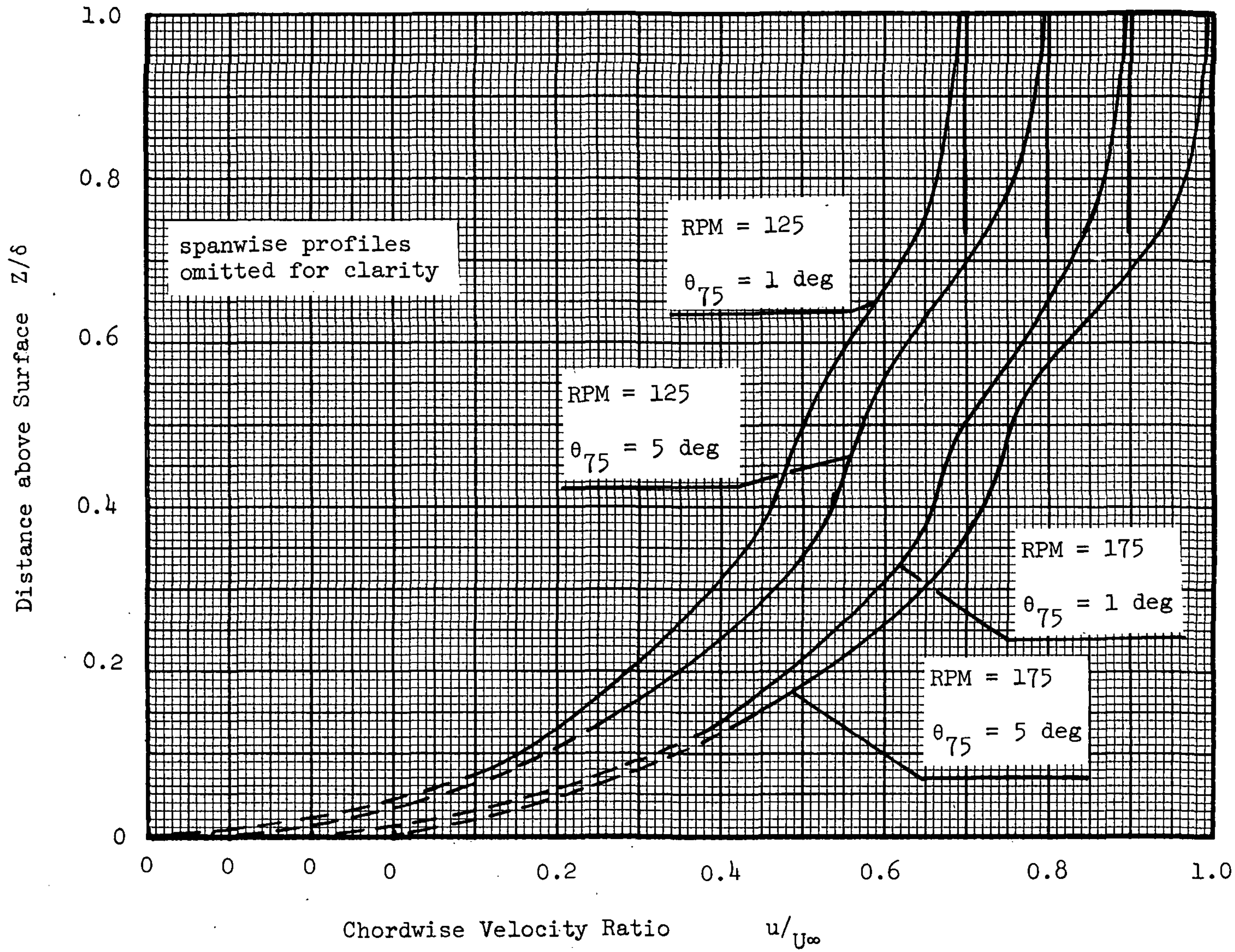

Figure 13. Typical Chordwise Velocity Profiles - Nondimensionalized.

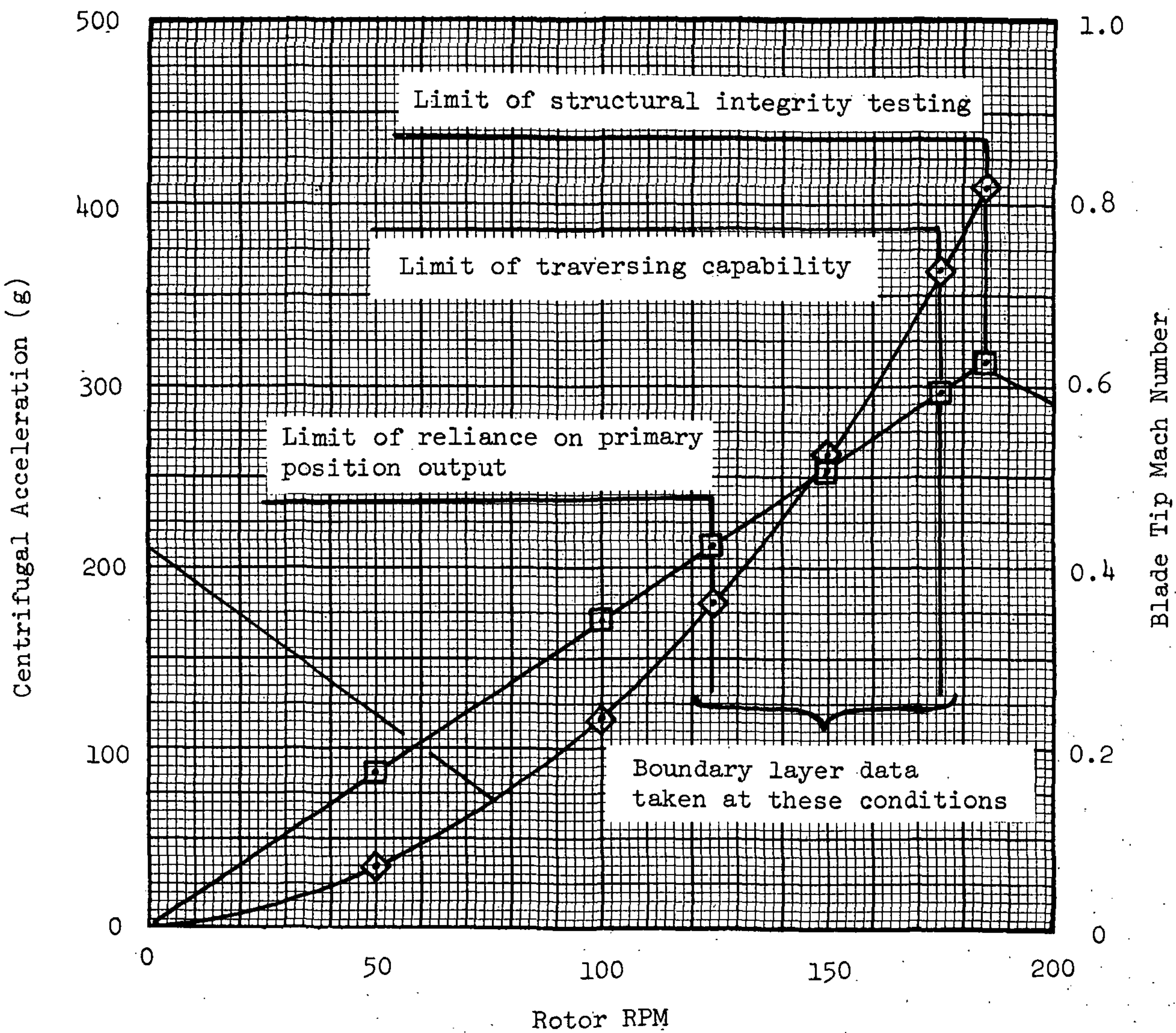

Figure 14. Summary of Test Conditions

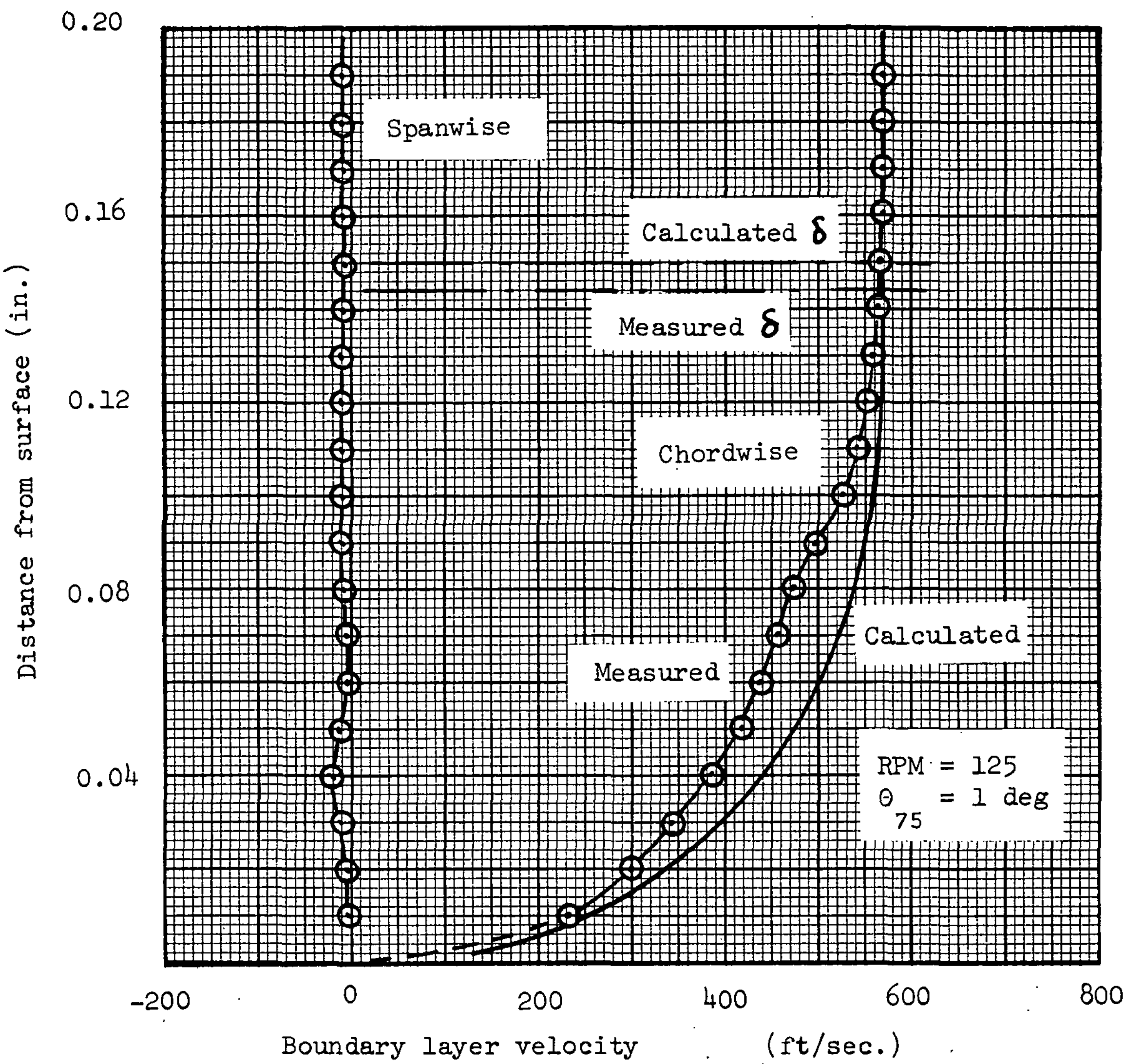

Figure 15. Comparison of Measured and Calculated, Reference 10, Velocity Profiles.

DISTRIBUTION LIST

	No. Copies
NASA Langley Research Center Hampton, VA 23365	
Attn: 122/Report & Manuscript Control Office	1
115/Raymond L. Zavasky	1
249/Warren H. Young, Jr.	10
NASA Ames Research Center Moffett Field, CA 94035 Attn: 202-3/Library	1
NASA Flight Research Center P. O. Box 273 Edwards, CA 93523 Attn: Library	1
NASA Goddard Space Flight Center Greenbelt, MD 20771 Attn: Library	1
NASA Manned Spacecraft Center 2101 Webster Seabrook Road Houston, TX 77058 Attn: JM6/Library	1
NASA Marshall Space Flight Center Huntsville, AL 35812 Attn: 111-113/Library	1
NASA Lewis Research Center 21000 Brookpark Road Cleveland, OH 44135 Attn: 60-3/Library	1
Jet Propulsion Laboratory 4800 Oak Grove Drive Pasadena, CA 91103 Attn: 111-113/Library	1
NASA John F. Kennedy Space Center Kennedy Space Center, FL 32899 Attn: IS-DOC-12L/Library	1
National Aeronautics & Space Administration Washington, DC 20546 Attn: KSS-10/Library	1
RA/NASA Headquarters	1

NASA CR-112194

DISTRIBUTION LIST

	No. Copies
NASA Army Aeronautical Research Laboratory NASA Ames Research Center Moffett Field, CA 94035 Attn: 207-5/Paul F. Yaggy 215-1/William James McCroskey	 1 1
Massachusetts Institute of Technology Department of Aeronatuics & Astronautics Aeroelastic & Structures Research Laboratory Cambridge, MA 02139 Attn: Dr. Norman D. Ham	 1
U. S. Naval Postgraduate School Monterey, CA 93940 Attn: Dr. J. A. Miller	 1
University of Virginia Aerospace Engineering Department Charlottesville, VA 23069 Attn: George T. Matthews	 1
Johns Hopkins University Department of Mechanics Baltimore, MD 21218 Attn: Dr. William G. Rose	 1
Ohio State University 2101 Robinson Laboratory Columbus, OH 43210 Attn: Prof. H. R. Velkoff	 1
U. S. Army Aviation Material Laboratories Aeromechanics Division Fort Eustis, VA 23603 Attn: John Yeates	 1
Bell Helicopter Company P. O. Box 482 Fort Worth, TX 76101 Attn: Watson Tanner	 1

NASA CR-112194

DISTRIBUTION LIST

	No. Copies
The Boeing Company Vertol Division P. O. Box 16858 Philadelphia, PA 19142 Attn: Frank Harris	1
NASA Scientific & Technical Information Facility P. O. Box 33 College Park, MD 20740	13

Sikorsky Aircraft DIVISION OF UNITED AIRCRAFT CORPORATION

STRATFORD, CONNECTICUT 06602

PHONE (203) 378-6361

SEL - 2588 December 13, 1972

National Aeronautics and Space Administration
Scientific & Technical Information Facility
P. O. Box 33
College Park, Maryland 20740

Subject: NASA Contract NAS1-11213
"Rotor Blade Boundary Layer Measurement - Hardware Feasability Demonstration"
Final Report NASA CR-112194

Enclosures: (1) Thirteen (13) copies of final report plus (1) reproducible copy. (Addressee only)
(2) Distribution List
(3) Assigned copies of Final Report (per enclosure 2)

Gentlemen,

Please find enclosed the final report on NASA contract NAS1-11213 "Rotor Blade Boundary Measurement Hardware Feasability Demonstration", NASA CR-112194. This is the final submittal of data under the subject contract.

Respectfully,

SIKORSKY AIRCRAFT

D. R. Clark

D. R. Clark
Program Manager

DRC:lb

cc: William R. Kivett, Contracting Officer
National Aeronautics & Space Administration
Langley Research Center
Hampton, Va., 23365
Enclosure (2) only

	No. Copies
NASA Langley Research Center Hampton, VA 23365	
Attn: 122/Report & Manuscript Control Office	1
115/Raymond L. Zavasky	1
249/Warren H. Young, Jr.	10
NASA Ames Research Center Moffett Field, CA 94035 Attn: 202-3/Library	1
NASA Flight Research Center P. O. Box 273 Edwards, CA 93523	1
NASA Goddard Space Flight Center Greenbelt, MD 20771 Attn: Library	1
NASA Manned Spacecraft Center 2101 Webster Seabrook Road Houston, TX 77058 Attn: JM6/Library	1
NASA Marshall Space Flight Center Huntsville, AL 35812 Attn: 111-113/Library	1
NASA Lewis Research Center 21000 Brookpark Road Cleveland, OH 44135 Attn: 60-3/Library	1
Jet Propulsion Laboratory 4800 Oak Grove Drive Pasadena, CA 91103 Attn: 111-113/Library	1
NASA John F. Kennedy Space Center Kennedy Space Center, FL 32899 Attn: IS-DOC-12L/Library	1
National Aeronautics & Space Administration Washington, DC 20546	
Attn: KSS-10/Library	1
RA/NASA Headquarters	1
NASA Army Aeronautical Research Laboratory NASA Ames Research Center Moffett Field, CA 94035	
Attn: 207-5/Paul F. Yaggy	1
215-1/William James McCroskey	1
215-1/Prof. H. R. Velkoff	1
215-1/Larry Carr	1

	No. Copies
Massachusetts Institute of Technology Department of Aeronautics & Astronautics Aeroelastic & Structures Research Laboratory Cambridge, MA 02139 Attn: Dr. Norman D. Ham	1
U. S. Naval Postgraduate School Monterey, CA 93940 Attn: Dr. J. A. Miller	1
University of Virginia Aerospace Engineering Department Charlottesville, Va 23069 Attn: George T. Matthews	1
Johns Hopkins University Department of Mechanics Baltimore, MD 21218 Attn: Dr. William G. Rose	1
U. S. Army Aviation Material Laboratories Aeromechanics Division Fort Eustis, VA 23603 Attn: John Yeates	1
Bell Helicopter Company P. O. Box 482 Fort Worth, TX 76101 Attn: Watson Tanner	1
The Boeing Company Vertol Division P. O. Box 16858 Philadelphia, PA 19142 Attn: Frank Harris	1
NASA Scientific & Technical Information Facility P. O. Box 33 College Park, MD 20740	13 plus reproducible